

On the Chermnykh-Like Problems:

II. The Equilibrium Points

Li-Chin Yeh¹ and Ing-Guey Jiang²

¹ Department of Applied Mathematics,

National Hsinchu University of Education, Hsin-Chu, Taiwan

² Institute of Astronomy,

National Central University, Chung-Li, Taiwan

Received _____; accepted _____

ABSTRACT

Motivated by Papadakis (2005a, 2005b), we study a Chermnykh-like problem, in which an additional gravitational potential from the belt is included. In addition to the usual five equilibrium points (three collinear and two triangular points), there are some new equilibrium points for this system. We studied the conditions for the existence of these new equilibrium points both analytically and numerically.

1. Introduction

The interest in the Chermnykh's problem (Chermnykh 1987) has been renewed by K.E. Papadakis recently. For example, Papadakis (2004) studied the symmetric motions near the three collinear equilibrium points in three dimensional space. Papadakis (2005a) numerically investigated the equilibrium points and the zero-velocity curves under the assumption that the mass parameter is fixed but the angular velocity parameter is allowed to vary continuously. The stability of the periodic orbits are determined and the network of the orbital families is explored.

Moreover, Papadakis (2005b) numerically studied the asymmetric periodic orbits near the triangular equilibrium points under the assumption that the angular velocity varies and for the Sun-Jupiter mass distribution. Remarkably, that paper provides the analytic determination of the initial conditions of the long- and short-period Trojan families around the equilibrium points.

On the other hand, astronomers claimed that it is common to have circumbinary discs for binary systems and asteroid belts for planetary systems. Some studies showed that these belt-like structures shall influence the mathematical properties of these dynamical systems. The number and locations of equilibrium points and also topology of solution curves might become very different when the influence from the belt is considered. For example, Jiang & Yeh (2003, 2004) considered the influence from the belt for planetary systems and found that the probability to have equilibrium points around the inner part of the belt is larger than the one near the outer part. Their results can be used to explain the observational configuration of Kuiper Belt Objects of the outer Solar System.

Jiang & Yeh (2006) have studied a Chermnykh-like problem in which the mass parameter μ is set to be 0.5. We now study the systems with any possible mass-ratio of central binaries both analytically and numerically. We will focus on conditions with which

the new equilibrium points can exist for two different density models of the belts. We can then understand the locations of these new equilibrium points for given parameters. We present our models in Section 2, the results for the existence of new equilibrium points are in Section 3. Section 4 is about the stability analysis and Section 5 concludes the paper.

2. The Models

We consider the motion of a test particle influenced by the gravitational force from the central binary and the circumbinary belt. We assume that two masses of the central binary are m_1 and m_2 and choose the unit of mass to make $G(m_1 + m_2) = 1$. If we define that

$$\mu = \frac{m_2}{m_1 + m_2},$$

then the two masses are $\mu_1 = Gm_1 = 1 - \mu$ and $\mu_2 = Gm_2 = \mu$. The separation of central binary objects is set to be unity. In this paper, we assume that $\mu \leq 0.5$. The location of two masses are always at $(1 - \mu, 0, 0)$ and $(-\mu, 0, 0)$.

The equation of motion is (Jiang & Yeh 2006)

$$\left\{ \begin{array}{l} \frac{dx}{dt} = u \\ \frac{dy}{dt} = v \\ \frac{du}{dt} = 2nv - \frac{\partial U^*}{\partial x} - \frac{\partial V}{\partial x} \\ \frac{dv}{dt} = -2nu - \frac{\partial U^*}{\partial y} - \frac{\partial V}{\partial y}, \end{array} \right. \quad (1)$$

where n is the central binary's angular velocity (Please note that we keep n as a parameter from here until Property 3.2 but set it to be 1 as a simplification starting from Eq.(20), i.e, Section 3.1 Model A.),

$$U^* = -\frac{n^2}{2}(x^2 + y^2) - \frac{1 - \mu}{r_1} - \frac{\mu}{r_2}, \quad (2)$$

$$r_1 = \sqrt{(x + \mu)^2 + y^2}, \quad (3)$$

$$r_2 = \sqrt{(x + \mu - 1)^2 + y^2} \quad (4)$$

and V is the potential from the belt. We assume that V is radial symmetric, so V depends on the radial distance r , where $r = \sqrt{x^2 + y^2}$. Hence,

$$\left\{ \begin{array}{l} \frac{\partial V}{\partial x} = \frac{x}{r} \frac{\partial V}{\partial r} \\ \frac{\partial V}{\partial y} = \frac{y}{r} \frac{\partial V}{\partial r}, \end{array} \right. \quad (5)$$

We substitute Eq. (2) and Eq. (5) into Eq.(1) and have the following system:

$$\left\{ \begin{array}{l} \frac{dx}{dt} = u \\ \frac{dy}{dt} = v \\ \frac{du}{dt} = 2nv + n^2x - \frac{(1-\mu)(x+\mu)}{r_1^3} - \frac{\mu(x+\mu-1)}{r_2^3} - \frac{x}{r} \frac{\partial V}{\partial r} \\ \frac{dv}{dt} = -2nu + n^2y - \frac{y(1-\mu)}{r_1^3} - \frac{y\mu}{r_2^3} - \frac{y}{r} \frac{\partial V}{\partial r}, \end{array} \right. \quad (6)$$

where r_1 and r_2 are defined in Eqs.(3)-(4). We can consider any density profile of the belt by giving a formula of V in Eq. (6) as long as V is radial symmetric. In this paper, we study two different models of the belt.

2.1. Model A: Miyamoto-Nagai Profile

In Model A, we introduce the belt potential, from Miyamoto & Nagai (1975), which is

$$V(r, z) = -\frac{M_b}{\sqrt{r^2 + (a + \sqrt{z^2 + b^2})^2}}, \quad (7)$$

where M_b is the total mass of the belt and $r^2 = x^2 + y^2$. In this formula, a and b are parameters which determine the density profile of the belt. The parameter a controls the flatness of the profile and can be called “flatness parameter”. The parameter b controls the size of the core of the density profile and can be called “core parameter”. When $a = b = 0$, the potential equals to the one by a point mass. In general, the density distribution

corresponding to the above $V(r, z)$ in Eq.(7) is, as in Miyamoto & Nagai (1975),

$$\rho(r, z) = \left(\frac{b^2 M_b}{4\pi} \right) \frac{ar^2 + (a + 3\sqrt{z^2 + b^2})(a + \sqrt{z^2 + b^2})^2}{[r^2 + (a + \sqrt{z^2 + b^2})^2]^{5/2}(z^2 + b^2)^{3/2}}. \quad (8)$$

If we define $T \equiv a + b$, from Eq. (7) we have

$$\frac{\partial V}{\partial r}(r, 0) = \frac{M_b r}{(r^2 + (a + b)^2)^{3/2}} = \frac{M_b r}{(r^2 + T^2)^{3/2}}, \quad (9)$$

where we set $z = 0$ since we only consider the orbits on the $x - y$ plane. We substitute Eq. (9) into Eq. (6) and have the following system:

$$\left\{ \begin{array}{l} \frac{dx}{dt} = u \\ \frac{dy}{dt} = v \\ \frac{du}{dt} = 2nv + n^2 x - \frac{(1-\mu)(x+\mu)}{r_1^3} - \frac{\mu(x+\mu-1)}{r_2^3} - \frac{M_b x}{(r^2+T^2)^{3/2}} \\ \frac{dv}{dt} = -2nu + n^2 y - \frac{y(1-\mu)}{r_1^3} - \frac{y\mu}{r_2^3} - \frac{M_b y}{(r^2+T^2)^{3/2}}. \end{array} \right. \quad (10)$$

We can see that neither the core parameter or the flatness parameter appear in the equations of motion. The dynamics of the system only depends on the summation of a and b , i.e. T .

2.2. Model B: Power-Law Profile

The belt is a annulus with inner radius r_i and outer radius r_o , where r_i and r_o are assumed to be constants. The density profile of the belt is

$$\rho(r) = \begin{cases} 0 & \text{when } r < r_i \text{ or } r > r_o, \\ \frac{c}{r^p} \left\{ \cos \left[\frac{\pi}{2} \frac{(r-r_1)}{(r_i-r_1)} \right] \right\}^2 & \text{when } r_i < r < r_1, \\ \frac{c}{r^p} & \text{when } r_1 < r < r_2, \\ \frac{c}{r^p} \left\{ \cos \left[\frac{\pi}{2} \frac{(r-r_2)}{(r_o-r_2)} \right] \right\}^2 & \text{when } r_2 < r < r_o, \end{cases} \quad (11)$$

where $r = \sqrt{x^2 + y^2}$, c is a constant completely determined by the total mass of the belt and we set $p = 2$ (Lizano & Shu 1989), $r_1 = r_i + 0.1$, $r_2 = r_1 + 0.8$, and $r_o = r_2 + 0.1$ for all

numerical results. Hence, for $p = 2$, the total mass of the belt is

$$\begin{aligned} M_b = & \int_0^{2\pi} \int_{r_i}^{r_o} \rho(r') r' dr' d\phi = 2\pi c \left\{ \int_{r_i}^{r_1} \frac{1}{r'} \left\{ \cos \left[\frac{\pi (r - r_1)}{2 (r_i - r_1)} \right] \right\}^2 dr' + \ln(r_2/r_1) \right. \\ & \left. + \int_{r_2}^{r_o} \frac{1}{r'} \left\{ \cos \left[\frac{\pi (r - r_2)}{2 (r_o - r_2)} \right] \right\}^2 dr' \right\}. \end{aligned} \quad (12)$$

The gravitational force f_b from the belt is (Jiang & Yeh 2004)

$$f_b(r) = -\frac{\partial V}{\partial r} = -2 \int_{r_i}^{r_o} \frac{\rho(r') r'}{r} \left[\frac{E(\xi)}{r - r'} + \frac{F(\xi)}{r + r'} \right] dr', \quad (13)$$

where $\xi = 2\sqrt{rr'}/(r + r')$, F and E are elliptic integrals of the first kind and the second kind. We substitute Eq. (13) into Eq.(6) and have the following system:

$$\left\{ \begin{array}{l} \frac{dx}{dt} = u \\ \frac{dy}{dt} = v \\ \frac{du}{dt} = 2nv + n^2x - \frac{(1-\mu)(x+\mu)}{r_1^3} - \frac{\mu(x+\mu-1)}{r_2^3} - \frac{2x}{r^2} \int_{r_i}^{r_o} \rho(r') r' \left[\frac{E}{r-r'} + \frac{F}{r+r'} \right] dr' \\ \frac{dv}{dt} = -2nu + n^2y - \frac{y(1-\mu)}{r_1^3} - \frac{y\mu}{r_2^3} - \frac{2y}{r^2} \int_{r_i}^{r_o} \rho(r') r' \left[\frac{E}{r-r'} + \frac{F}{r+r'} \right] dr'. \end{array} \right. \quad (14)$$

3. The New Equilibrium Points

It is well-known that there are five equilibrium points, i.e. three collinear and two triangular points, for the classical restricted three-body problem. When there are more than five equilibrium points for the system we study here, we claim that the new equilibrium points exist.

In general, for System (6), equilibrium points (x_e, y_e) satisfies $f(x_e, y_e) = 0$ and $g(x_e, y_e) = 0$, where

$$f(x, y) = n^2x - \frac{(1-\mu)(x+\mu)}{r_1^3} - \frac{\mu(x+\mu-1)}{r_2^3} - \frac{x}{r} \frac{\partial V}{\partial r}, \quad (15)$$

$$g(x, y) = n^2y - \frac{y(1-\mu)}{r_1^3} - \frac{y\mu}{r_2^3} - \frac{y}{r} \frac{\partial V}{\partial r}. \quad (16)$$

For convenience, we define

$$h(y) \equiv n^2 - \left[\frac{1}{4} + y^2 \right]^{-3/2} - \frac{1}{r} \frac{\partial V}{\partial r} \Big|_{(\frac{1}{2} - \mu, y)} \quad (17)$$

and

$$k(x) \equiv n^2 x - \frac{(1 - \mu)(x + \mu)}{|x + \mu|^3} - \frac{\mu(x + \mu - 1)}{|x + \mu - 1|^3} - \frac{x}{r} \frac{\partial V}{\partial r} \Big|_{(x, 0)}. \quad (18)$$

We have the following properties:

Property 3.1

If (x_e, y_e) is an equilibrium point of System (6), then we have

either (1) $x_e = 1/2 - \mu$ and y_e satisfies $h(y) = 0$

or (2) x_e satisfies $k(x) = 0$ and $y_e = 0$.

Proof: Suppose that (x_e, y_e) is an equilibrium point, thus it satisfies $f(x, y) = 0$ and $g(x, y) = 0$. From Eq.(16), we have

$$y_e \left[n^2 - \frac{1 - \mu}{r_1^3} - \frac{\mu}{r_2^3} - \frac{1}{r} \frac{\partial V}{\partial r} \right]_{(x_e, y_e)} = 0.$$

Hence, $y_e = 0$ or $n^2 - \frac{1 - \mu}{r_1^3} - \frac{\mu}{r_2^3} - \frac{1}{r} \frac{\partial V}{\partial r} \Big|_{(x_e, y_e)} = 0$. We discuss these two cases separately:

$$(I) \quad n^2 - \frac{1 - \mu}{r_1^3} - \frac{\mu}{r_2^3} - \frac{1}{r} \frac{\partial V}{\partial r} \Big|_{(x_e, y_e)} = 0:$$

Since (x_e, y_e) is an equilibrium point, that is $f(x_e, y_e) = 0$, we have

$$0 = f(x_e, y_e) = x_e \left[n^2 - \frac{1 - \mu}{r_1^3} - \frac{\mu}{r_2^3} - \frac{1}{r} \frac{\partial V}{\partial r} \right] - \frac{(1 - \mu)\mu}{r_1^3} + \frac{(1 - \mu)\mu}{r_2^3} = (1 - \mu)\mu \left[-\frac{1}{r_1^3} + \frac{1}{r_2^3} \right]. \quad (19)$$

Thus, $r_1 = r_2$, i.e. $(x_e + \mu)^2 + y_e^2 = (x_e + \mu - 1)^2 + y_e^2$. Hence $x_e = 1/2 - \mu$. We have $r_1 = r_2 = \sqrt{1/4 + y_e^2}$ and thus, $n^2 - \frac{1 - \mu}{r_1^3} - \frac{\mu}{r_2^3} = n^2 - \left[\frac{1}{4} + y_e^2 \right]^{-3/2}$. Therefore, $x_e = 1/2 - \mu$ and y_e satisfies $h(y) = 0$ for the equilibrium point (x_e, y_e) .

(II) $y_e = 0$:

$f(x_e, y_e) = f(x_e, 0) = k(x_e) = 0$ for the equilibrium point (x_e, y_e) . Thus, x_e satisfies $k(x) = 0$ and $y_e = 0$. \square

Property 3.2

(A) If y_e satisfies $h(y) = 0$, then $(1/2 - \mu, y_e)$ is the equilibrium point of System (6).

(B) If x_e satisfies $k(x) = 0$, then $(x_e, 0)$ is the equilibrium point of System (6).

Proof of (A): Suppose that y_e is one of the roots of $h(y)$, i.e. $h(y_e) = 0$ and we set $x_e = 1/2 - \mu$. Because $g(1/2 - \mu, y_e) = y_e h(y_e) = 0$ and $f(1/2 - \mu, y_e) = \left(\frac{1}{2} - \mu\right) h(y_e) = 0$, (x_e, y_e) is the equilibrium point of System (6). \square

Proof of (B): Suppose that x_e is one of the roots of $k(x)$, i.e. $k(x_e) = 0$ and we set $y_e = 0$. Since $y_e = 0$, it is trivial that $g(x_e, y_e) = 0$. Because $k(x_e) = 0$, $f(x_e, 0) = k(x_e) = 0$. Thus, (x_e, y_e) is the equilibrium point of System (6). \square

Because of the above two properties, in stead of searching the roots for two variable functions $f(x, y)$ and $g(x, y)$ to determine all equilibrium points on the $x - y$ plane, we only need to find the roots of one variable functions $h(y)$ and $k(x)$ to get all the equilibrium points of System (6).

3.1. Model A

We now study the equilibrium points when V is Miyamoto-Nagai profile. From Property 3.1, equilibrium points should be either on the x -axis or on the line: $x = 1/2 - \mu$ of $x - y$ plane. As a simplification, please note that we set $n = 1$ hereafter. For equilibrium points on the x -axis, i.e. $(x_e, 0)$, we have

$$k(x_e) = x_e - \frac{(1 - \mu)(x_e + \mu)}{|x_e + \mu|^3} - \frac{\mu(x_e + \mu - 1)}{|x_e + \mu - 1|^3} - \frac{x_e M_b}{(x_e^2 + T^2)^{3/2}} = 0. \quad (20)$$

On the other hand, for those equilibrium points on the line: $x = 1/2 - \mu$ (i.e. $(1/2 - \mu, y_e)$), and thus $r = \sqrt{(1/2 - \mu)^2 + y_e^2}$, we have

$$h(y_e) = 1 - \left[\frac{1}{4} + y_e^2 \right]^{-3/2} - M_b \left[\left(\frac{1}{2} - \mu \right)^2 + y_e^2 + T^2 \right]^{-3/2} = 0. \quad (21)$$

Property 3.3

There is one and only one $\bar{y}_1 > 0$ such that $h(\bar{y}_1) = 0$, and only one $\bar{y}_2 < 0$ such that $h(\bar{y}_2) = 0$. That is, there are two equilibrium points on the line: $x = 1/2 - \mu$ for System (10).

Proof: We define

$$P_1(y) = \left[\frac{1}{4} + y^2 \right]^{-3/2} - 1 \quad (22)$$

$$\text{and} \quad Q_1(y) = -M_b \left[\left(\frac{1}{2} - \mu \right)^2 + y^2 + T^2 \right]^{-3/2}, \quad (23)$$

so from Eq.(21), we have

$$h(y) = 1 - \left[\frac{1}{4} + y^2 \right]^{-3/2} - M_b \left[\left(\frac{1}{2} - \mu \right)^2 + y^2 + T^2 \right]^{-3/2} \equiv -P_1(y) + Q_1(y) = 0. \quad (24)$$

From Eqs. (22)-(23), we have

$$Q'_1(y) = 3yM_b \left[\left(\frac{1}{2} - \mu \right)^2 + y^2 + T^2 \right]^{-5/2} \quad \text{and} \quad P'_1(y) = -3y \left[\frac{1}{4} + y^2 \right]^{-5/2}.$$

Since $P'_1(y) < 0$ for $y > 0$, $P_1(y)$ is a monotonically decreasing and continuous function for any $y \in (0, \infty)$. $Q'_1(y) > 0$ for $y > 0$, thus $Q_1(y)$ is a monotonically increasing and continuous function for any $y \in (0, \infty)$. Because $P_1(0) > 0 > Q_1(0)$ and $\lim_{y \rightarrow \infty} P_1(y) < \lim_{y \rightarrow \infty} Q_1(y)$, there exists a unique point $\bar{y}_1 > 0$ such that $P_1(\bar{y}_1) = Q_1(\bar{y}_1)$, that is $h(\bar{y}_1) = 0$.

By the similar method, we find that there is a unique point $\bar{y}_2 < 0$ such that $h(\bar{y}_2) = 0$.

Hence, there are two equilibrium points on the line: $x = 1/2 - \mu$. \square

In the classical restricted three-body problem, there are three collinear points and two triangular points, i.e. the points on the line: $x = 1/2 - \mu$. Therefore, Property 3.3 shows that there is no new equilibrium points on the line: $x = 1/2 - \mu$ for Model A. If there is any new equilibrium points for this model, it must be on the x -axis.

Let

$$P_2(x) = \frac{(1 - \mu)(x + \mu)}{|x + \mu|^3} + \frac{\mu(x + \mu - 1)}{|x + \mu - 1|^3} - x, \quad (25)$$

and thus,

$$P_2(x) = \begin{cases} \frac{1-\mu}{(x+\mu)^2} + \frac{\mu}{(x+\mu-1)^2} - x, & \text{for } x > 1 - \mu, \\ \frac{(1-\mu)}{(x+\mu)^2} - \frac{\mu}{(x+\mu-1)^2} - x, & \text{for } -\mu < x < 1 - \mu, \\ -\frac{1-\mu}{(x+\mu)^2} - \frac{\mu}{(x+\mu-1)^2} - x, & \text{for } x < -\mu. \end{cases} \quad (26)$$

We also set

$$Q_2(x) = -\frac{xM_b}{(x^2 + T^2)^{3/2}}. \quad (27)$$

It is obvious that $P_2(x)$ contains the terms related to the gravitational forces from the central binary and the centrifugal force. $Q_2(x)$ is simply the term contributed by the belt. By defining these two functions, we have both the advantages that the physical meanings are clear and some properties about the new equilibrium can be proved easily.

From Eq.(20), we have $f(x, 0) = k(x) = -P_2(x) + Q_2(x)$. The equilibrium points $(x_e, 0)$ satisfy $f(x_e, 0) = k(x_e) = 0$, that is, $P_2(x_e) = Q_2(x_e)$. There are two properties for this part of our results: Property 3.4 is for the case of non-equal mass binaries, i.e. $0.5 > \mu > 0$ and Property 3.5 is for the case of equal mass binaries, i.e. $\mu = 0.5$. In Property 3.4, we find that there are three equilibrium points, $(x_i, 0)$ for $i = 1, 2, 3$, where $x_1 \in (-\infty, -\mu)$, $x_2 \in (0, 1 - \mu)$ and $x_3 \in (1 - \mu, \infty)$. However, the results for the equilibrium points which x -coordinate is in the region $(-\mu, 0)$ are more complicated. As we can see in Property 3.4 (C), there are two equilibrium points which x -coordinates are in the region $(-\mu, 0)$, and in Property 3.4 (D), there is no equilibrium point with x -coordinate in the region $(-\mu, 0)$. We will see that, in fact, Property 3.5 (A) could be combined with Property 3.4 (B). However, Property 3.5 (B) studies the same condition as in Property 3.4 (C) but the results for that condition are completely different. Moreover, There is nothing like Property 3.4 (A) and 3.4 (D) in Property 3.5. These differences are due to that $P_2(-x) = -P_2(x)$ and $Q_2(-x) = -Q_2(x)$ when $\mu = 1/2$ but the symmetry is broken when $\mu < 1/2$. We therefore decided to separate Property 3.4 and 3.5. For convenience, we will denote μ^+ to represent that x tends to μ from the right hand side and μ^- to represent that x tends to μ from the

left hand side.

Property 3.4

- (A) *There is an $x_1 > 1 - \mu$ and an $x_2 \in (0, 1 - \mu)$ such that $k(x_1) = 0$ and $k(x_2) = 0$.*
- (B) *There is an $x_3 < -\mu$ such that $k(x_3) = 0$.*
- (C) *If $T < \sqrt{2}\mu$ and $Q_2(-T/\sqrt{2}) > P_2(-T/\sqrt{2})$, then there are two points in the region $(-\mu, 0)$ such that $k(x) = 0$.*
- (D) *If $Q_2(-T/\sqrt{2}) < P_2(0)$, then there is no point in the region $(-\mu, 0)$ such that $k(x) = 0$.*

Proof of (A): From Eqs. (25)-(27), we know that if $x > 1 - \mu$, then

$$P_2(x) = \frac{1 - \mu}{(x + \mu)^2} + \frac{\mu}{(x + \mu - 1)^2} - x, \quad (28)$$

and

$$P'_2(x) = -\frac{2(1 - \mu)}{(x + \mu)^3} - \frac{2\mu}{(x + \mu - 1)^3} - 1.$$

Since $P'_2(x) < 0$ for $x > 1 - \mu$, P_2 is a monotonically decreasing function for $x \in (1 - \mu, \infty)$. Because $\lim_{x \rightarrow (1 - \mu)^+} P_2(x) = \infty$, $\lim_{x \rightarrow \infty} P_2(x) = -\infty$ and $Q_2(1 - \mu) < 0$, $\lim_{x \rightarrow \infty} Q_2(x) = 0$, we have $\lim_{x \rightarrow (1 - \mu)^+} k(x) = \lim_{x \rightarrow (1 - \mu)^+} (-P_2(x) + Q_2(x)) < 0$ and $\lim_{x \rightarrow \infty} k(x) = \lim_{x \rightarrow \infty} (-P_2(x) + Q_2(x)) > 0$. Therefore, there is a point $x_1 > 1 - \mu$ such that $k(x_1) = 0$.

In the region $(0, 1 - \mu)$, $P_2(0) > 0$, $\lim_{x \rightarrow (1 - \mu)^-} P_2(x) = -\infty$, $Q_2(0) = 0$ and $Q_2(1 - \mu) < 0$, so we have $k(0) = -P_2(0) + Q_2(0) < 0$ and $\lim_{x \rightarrow (1 - \mu)^-} k(x) = \infty$. Therefore, there is an $x_2 \in (0, 1 - \mu)$ such that $k(x_2) = 0$. \square

Proof of (B): If $x < -\mu$, then

$$P_2(x) = -\frac{1 - \mu}{(x + \mu)^2} - \frac{\mu}{(x + \mu - 1)^2} - x.$$

Since $P'_2(x) < 0$ for $x < -\mu$, P_2 is a monotonically decreasing function for $x < -\mu$.

Because $\lim_{x \rightarrow -\mu^-} P_2(x) = -\infty$, $\lim_{x \rightarrow -\infty} P_2(x) = \infty$ and $Q_2(-\mu) > 0$,

$\lim_{x \rightarrow -\infty} Q_2(x) = 0$, we have $\lim_{x \rightarrow -\mu^-} k(x) > 0$ and $\lim_{x \rightarrow -\infty} k(x) < 0$. Therefore, there is a point $x_3 < -\mu$ such that $k(x_3) = 0$. \square

Proof of (C): If $x \in (-\mu, 0)$, then

$$P_2(x) = \frac{1-\mu}{(x+\mu)^2} - \frac{\mu}{(x+\mu-1)^2} - x.$$

If $T < \sqrt{2}\mu$, we have that $-\mu < -T/\sqrt{2}$. We then discuss the possible points such that $k(x) = 0$ for $x = -T/\sqrt{2}$, $x \in (-T/\sqrt{2}, 0)$ and $x \in (-\mu, -T/\sqrt{2})$ separately.

If $Q_2(-T/\sqrt{2}) > P_2(-T/\sqrt{2})$, then $k(-T/\sqrt{2}) = -P_2(-T/\sqrt{2}) + Q_2(-T/\sqrt{2}) > 0$. Thus, $k(x) \neq 0$ when $x = -T/\sqrt{2}$.

Because we set $0 < \mu < 0.5$ in this paper, we have $P_2(0) > 0$. Since $Q_2(0) = 0$, we have $k(0) = -P_2(0) + Q_2(0) < 0$. Further, if $Q_2(-T/\sqrt{2}) > P_2(-T/\sqrt{2})$, then $k(-T/\sqrt{2}) > 0$. Thus, there is an $x_4 \in (-T/\sqrt{2}, 0)$ such that $k(x_4) = 0$.

On the other hand, since $P'_2(x) < 0$, $Q'_2(x) > 0$ for $x \in (-\mu, -T/\sqrt{2})$, $k'(x) > 0$ for $x \in (-\mu, -T/\sqrt{2})$. Thus, $k(x)$ is a monotonically increasing function. Because $\lim_{x \rightarrow -\mu^+} P_2(x) = \infty$ and $Q_2(-\mu) > 0$, we have $\lim_{x \rightarrow -\mu^+} k(x) < 0$. If $Q_2(-T/\sqrt{2}) > P_2(-T/\sqrt{2})$, then $k(-T/\sqrt{2}) > 0$. Therefore, there is a unique point $x_5 \in (-\mu, -T/\sqrt{2})$ such that $k(x_5) = 0$. \square

Proof of (D): Since $P'_2(x) < 0$ for $x \in (-\mu, 0)$, P_2 is a monotonically decreasing function and has a minimum value $P_2(0)$ in the region $(-\mu, 0)$. It is easy to show that $Q_2(-T/\sqrt{2})$ is the maximum value for $Q_2(x)$ in the region $(-\mu, 0)$. If $Q_2(-T/\sqrt{2}) < P_2(0)$, we have $P_2(x) > Q_2(x)$ and thus $k(x) < 0$ in the region $(-\mu, 0)$. Therefore, there is no point such that $k(x) = 0$ in the region $(-\mu, 0)$. \square

In Property 3.5, we study the $\mu = 1/2$ case. Since $P_2(-x) = -P_2(x)$ and $Q_2(-x) = -Q_2(x)$, we only need to discuss $(-\infty, 0)$ region.

Property 3.5

- (A) *There is an $x_1 < -1/2$ such that $k(x_1) = 0$.*
- (B) *If $T < 1/\sqrt{2}$ and $Q_2(-T/\sqrt{2}) > P_2(-T/\sqrt{2})$, then there is a point in the region $(-1/2, -T/\sqrt{2})$ such that $k(x) = 0$.*

Proof : (A) can be proved easily by the the same method as the proof for Property 3.4 (B). In the following, we would like to prove (B). Since $Q_2(-T/\sqrt{2}) > P_2(-T/\sqrt{2})$, $k(-T/\sqrt{2}) > 0$. Since $Q_2(-1/2)$ is finite and $\lim_{x \rightarrow (-1/2)^+} P_2(x) = \infty$, $\lim_{x \rightarrow (-1/2)^+} k(x) < 0$. Thus, there is a point $x^* \in (-1/2, -T/\sqrt{2})$ such that $k(x^*) = 0$. \square

From Property 3.5, if $T < 1/\sqrt{2}$ and $Q_2(-T/\sqrt{2}) > P_2(-T/\sqrt{2})$, we could have two points such that $k(x) = 0$ in the region $(-\infty, 0)$. By the property of symmetry, we will have another two roots in the region $(0, \infty)$. Since $k(0) = 0$, there are at least five points such that $k(x) = 0$ for the equal mass case. We know that there are only three equilibrium points on the x -axis for the classical restricted three-body problem, thus new equilibrium points exist for this case. From Property 3.3, 3.4 and Property 3.5, we have the following corollary to analytically determine the area which certainly have new equilibrium points for both $0 < \mu < 0.5$ and $\mu = 0.5$ cases.

Corollary 3.6

If $T < \sqrt{2}\mu$ and $Q_2(-T/\sqrt{2}) > P_2(-T/\sqrt{2})$, then we will have new equilibrium points.

That is, there are at least five equilibrium points on the x -axis for System (10).

One can see that the conditions studied in Property 3.4 and 3.5 do not include all possible cases. That is, there are some conditions we fail to provide analytical results due to that the results of those cases would more strongly depend on the detail structure of the function $P_2(x)$ and $Q_2(x)$. Thus, Corollary 3.6 shows that the condition, $T < \sqrt{2}\mu$ and $Q_2(-T/\sqrt{2}) > P_2(-T/\sqrt{2})$, is only a sufficient condition to have new equilibrium points. It is not a necessary condition.

To check the above statements, we numerically solve both Eq.(20) and Eq. (21) and find out the number of equilibrium points for different given parameters. The numerical scheme of root finding is the Van Wijngaarden-Dekker-Brent Method (Brent 1973). This is an excellent algorithm recommended by Press et al. (1992). We set a high level of accuracy that the maximum error is 10^{-8} for the locations of equilibrium points on both x -axis and the line: $x = 1/2 - \mu$. All the new equilibrium points are on the x -axis as we have proved in the analytic results. Figure 1 is the results on the $\mu - M_b$ plane. That is, we numerically search the solutions of both Eq.(20) and Eq.(21) for different (μ, M_b) , where μ is between $[0, 0.5]$ and M_b is between $[0, 0.6]$. Those (μ, M_b) with new equilibrium points are marked by points.

In each panel, there is a solid curve which satisfies $Q_2(-T/\sqrt{2}) = P_2(-T/\sqrt{2})$ with given parameters. Figure 1(a) shows that this curve perfectly match the boundary of the existence area of new equilibrium points. Therefore, Corollary 3.6 precisely predicts our numerical results. However, as we mentioned earlier, our analytic results do not include all possible conditions. Thus, the solid curve and the boundary of the existence area of new equilibrium points do not match that well in Figure 1(b)-(d). We cannot see the solid curve in Figure 1(d) since this curve is out of our studied parameter space.

Moreover, Figure 1 shows that the area without any points are on the left-bottom of $\mu - M_b$ plane. This is reasonable since (1) when M_b is small, it becomes classical restricted three-body problem and (2) when μ is small, this system become similar to a planetary system with a belt.

From Figure 1(a), i.e. $T = 0.01$ case, it is interesting that there is a lower limit of mass ratio: below that ratio, there would be no new equilibrium point no matter how large the belt mass is. Such limits of mass ratio become larger for larger T as in Figure (b)-(d). In general, when the mass of the belt is larger, it is easier to have new equilibrium points for

larger mass ratio. It is interesting that the new equilibrium points could exist for the larger area on the $\mu - M_b$ plane when T is smaller. It is also interesting that the locations and number of equilibrium points depend on T but not directly on a and b . T is the summation of a (the flatness parameter) and b (the core parameter) and the Miyamoto-Nagai potential would be equivalent to the potential of a point mass when $T = 0$.

Figure 2 is the results on the $T - M_b$ plane. That is, we numerically search the solutions of both Eq.(20) and Eq.(21) for different (T, M_b) , where T is between $[0, 0.4]$ with grid size 0.01 and M_b is between $[0, 0.6]$ with grid size 0.02. Those (T, M_b) with new equilibrium points are marked by points.

Figure 2 shows that when T is small enough, we always have new equilibrium points for any value of belt mass. We also plot out the solid curve: $Q_2(-T/\sqrt{2}) = P_2(-T/\sqrt{2})$ in each panel. The left-up side of the solid curve satisfies the condition of Corollary 3.6, i.e. $Q_2(-T/\sqrt{2}) > P_2(-T/\sqrt{2})$, so we have new equilibrium points in this area. We find that these solid curves can match the boundaries of the existence area of new equilibrium points very well for Figure 2(a)-(c) but not that well for Figure 2(d). Nevertheless, they all indicate that our analytic results are completely consistent with our numerical results.

In addition to the full circle points, for the comparison purpose here, there are also open triangle points in Figure 2(d). The open triangle points are the results for $n = \sqrt{1 - 2f_b(0.5)}$ as in Jiang & Yeh (2006). The open triangle points almost cover the same area as the one covered by the full circle points, thus our simplification that $n = 1$ is a good approximation.

3.2. Model B

On the other hand, we also study Model B: Power-Law Profile. By Property 3.1, the equilibrium points (x_e, y_e) must be on the lines: $x = 1/2 - \mu$ or $y = 0$. Property 3.1 and 3.2

indicates that we only need to solve x_e from

$$k(x) = x - \frac{\mu_1(x + \mu_2)}{r_1^3} - \frac{\mu_2(x - \mu_1)}{r_2^3} - \frac{2x}{r^2} \int_{r_i}^{r_o} \rho(r') r' \left[\frac{E}{r - r'} + \frac{F}{r + r'} \right] dr' \Big|_{y=0} = 0 \quad (29)$$

and y_e from

$$h(y) = 1 - \left[\frac{1}{4} + y^2 \right]^{-3/2} - \frac{2}{r^2} \int_{r_i}^{r_o} \rho(r') r' \left[\frac{E}{r - r'} + \frac{F}{r + r'} \right] dr' \Big|_{x=(\mu_1-\mu_2)/2} = 0 \quad (30)$$

to get all the equilibrium points $(x_e, 0)$ and $(1/2 - \mu, y_e)$. Because there are Elliptic Integrals in $k(x)$ and $h(y)$, it is very difficult to get any analytic results as Property 3.3, 3.4 and 3.5 of Model A. Thus, we try to find the roots of $k(x)$ and $h(y)$ numerically and we only present the numerical results here. The numerical method is exactly the same as the one used in Model A.

Contrary to Model A, we find that the new equilibrium points can exist both on the vertical line: $x = 1/2 - \mu$ and on the x -axis. Figure 3 and Figure 4 are the results, where the cross points are those area when there are more than three roots for $k(x) = 0$, the circles are the area when there are more than two roots for $h(y) = 0$. Please note that for the classical restricted three-body problem, there are three collinear points and two triangular ones.

Figure 3 is the results on the $\mu - M_b$ plane. That is, we numerically search the solutions of both Eq.(20) and Eq.(21) for different (μ, M_b) , where μ is between $[0, 0.5]$ and M_b is between $[0, 0.6]$.

The area of circles in Figure 3(a) looks like a square, thus there is a lower limit of mass ratio that no matter how large the belt mass is, there would be no new equilibrium point. There is also a lower limit of belt mass that no matter what mass ratio is, there would be no new equilibrium point. Figure 3(b) and (c) are very similar but the area becomes more like a quarter of a circle. The existence area of new equilibrium points in Figure 3(d) is very different from others.

The cross points in Figure 3 only appear for a small range of mass ratio. That is, with the additional force from the belt, the mass ratio has to be a particular value to have new equilibrium points. This means that it is more difficult to have new equilibrium points on the x -axis than that on the y -axis. To have new equilibrium points on the y -axis, the centrifugal force has to balance with the y -component of the total force from both central binary objects plus the force from the belt. That is, there are three components to balance each other at the equilibrium points and the mass ratio would only modify the locations of equilibrium points. However, on the x -axis, the forces from two central binary objects are in different directions at new equilibrium points, thus there are four components to balance each other for this case. Therefore, it will be more difficult for them to get balanced. To have new equilibrium points, the mass ratio has to be within a particular range.

Figure 4 is the results on the $r_i - M_b$ plane. That is, we numerically search the solutions of both Eq.(20) and Eq.(21) for different (r_i, M_b) , where r_i is between $[0,1]$ with grid size 0.01 and M_b is between $[0, 0.6]$ with grid size 0.02.

The cross points in Figure 4 show that there is a gap of r_i where it is more difficult to have new equilibrium points on the x -axis. It seems that this gap become larger when μ is larger. The reason why it would be more difficult to have new equilibrium points for particular region of r_i might be related to the relative positions of central binary objects with respect to the belt. The number of separate components which could balance each other might influence the existence of new equilibrium points.

The circles in Figure 4 are very interesting. In Figure 4(a) where the mass ratio is $\mu = 1/11$, there is a triangle area, i.e. when $0.5 < r_i < 0.8$, the range of belt mass to have new equilibrium points is larger if r_i is larger. However, when $r_i < 0.5$ or $r_i > 0.8$, there is no new equilibrium point. The triangle becomes slightly larger in Figure 4(b) and it becomes the combination of two trapezoids facing each other in Figures 4(c)-(d).

4. Stability Analysis

When the locations of equilibrium points are determined, it would be interesting to understand the stability properties around these points. We now consider the following system:

$$\left\{ \begin{array}{l} \frac{dx}{dt} = u \\ \frac{dy}{dt} = v \\ \frac{du}{dt} = 2v + f(x, y) \\ \frac{dv}{dt} = -2u + g(x, y), \end{array} \right. \quad (31)$$

where $f(x, y)$, $g(x, y)$ are defined in Eqs.(15)-(16). Following the usual linearization, the eigenvalues λ corresponding to the equilibrium points would satisfy:

$$\lambda^4 + (4 - f_x - g_y)\lambda^2 + 2(f_y - g_x)\lambda + f_x g_y - g_x f_y = 0, \quad (32)$$

where $f_x \equiv \partial f(x, y)/\partial x$ and f_y, g_x, g_y are also defined similarly.

Consider a new equilibrium point (x_e, y_e) of Model A as an example, so (x_e, y_e) satisfies $k(x_e) = 0$ and $y_e = 0$. Thus, we have:

$$\begin{aligned} f_x(x_e, 0) &= \left(\frac{\mu}{x_e} + 3 \right) \frac{1 - \mu}{|x_e + \mu|^3} - \left(\frac{1 - \mu}{x_e} + 3 \right) \frac{\mu}{|x_e + \mu - 1|^3} + \frac{3M_b x_e^2}{(x_e^2 + T^2)^{5/2}}, \\ g_y(x_e, 0) &= \frac{\mu(1 - \mu)}{x_e} \left(\frac{1}{|x_e - \mu|^3} - \frac{1}{|x_e + \mu - 1|^3} \right). \end{aligned} \quad (33)$$

Since $f_y(x_e, 0) = 0$ and $g_x(x_e, 0) = 0$, Eq.(32) becomes

$$\lambda^4 + (4 - f_x - g_y)\lambda^2 + f_x g_y = 0. \quad (34)$$

For convenience, we define $\Omega = f_x g_y$ and $\Pi = f_x + g_y - 4$. Therefore, we have

$$\lambda_+^2 = \frac{\Pi + \sqrt{\Pi^2 - 4\Omega}}{2} \quad \text{and} \quad \lambda_-^2 = \frac{\Pi - \sqrt{\Pi^2 - 4\Omega}}{2}. \quad (35)$$

These two relations will determine the eigenvalues and the properties of the equilibrium point. In fact, the signs of $\Pi^2 - 4\Omega$, $\Pi + \sqrt{\Pi^2 - 4\Omega}$, and $\Pi - \sqrt{\Pi^2 - 4\Omega}$ will completely

determine the results. However, when one knows the signs of Π and Ω , the details of possible eigenvalues can be directly determined by them. We therefore list all the combinations in Table 1, in terms of the signs of $\Pi^2 - 4\Omega$, Π and Ω .

Table 1. The Possible Combinations

Condition A	Condition B	Condition C	Row	λ_+^2	λ_-^2
$\Pi^2 - 4\Omega < 0$			1	c	c
$\Pi^2 - 4\Omega = 0$	$\Pi < 0$		2	–	–
$\Pi^2 - 4\Omega = 0$	$\Pi = 0$		3	0	0
$\Pi^2 - 4\Omega = 0$	$\Pi > 0$		4	+	+
$\Pi^2 - 4\Omega > 0$	$\Pi < 0$	$\Omega < 0$	5	+	–
$\Pi^2 - 4\Omega > 0$	$\Pi < 0$	$\Omega = 0$	6	0	–
$\Pi^2 - 4\Omega > 0$	$\Pi < 0$	$\Omega > 0$	7	–	–
$\Pi^2 - 4\Omega > 0$	$\Pi = 0$	$\Omega < 0$	8	+	–
$\Pi^2 - 4\Omega > 0$	$\Pi = 0$	$\Omega = 0$	9 (impossible)		
$\Pi^2 - 4\Omega > 0$	$\Pi = 0$	$\Omega > 0$	10 (impossible)		
$\Pi^2 - 4\Omega > 0$	$\Pi > 0$	$\Omega < 0$	11	+	–
$\Pi^2 - 4\Omega > 0$	$\Pi > 0$	$\Omega = 0$	12	+	0
$\Pi^2 - 4\Omega > 0$	$\Pi > 0$	$\Omega > 0$	13	+	+

In Row 1, due to $\Pi^2 - 4\Omega < 0$, λ_{\pm}^2 are then imaginary complex conjugate numbers. Thus, λ_{\pm} can be expressed as $\lambda_{\pm} = \pm a \pm bi$ and $\lambda_{\pm} = \pm c \pm di$, where a, b, c and d are positive real numbers. So in this case, the equilibrium point is an unstable point.

In Row 2, 3, and 4,

$$\lambda_{\pm}^2 = \lambda_{\pm}^2 = \frac{\Pi}{2}.$$

Thus, λ_{\pm} could be pure imaginary (Row 2), zeroes (Row 3) and $\pm\sqrt{\frac{\Pi}{2}}$ (Row 4). The

equilibrium point is neutrally stable for Row 2 and 3 but unstable for Row 4.

In Row 5, because $\Omega < 0$, we have $\Pi^2 - 4\Omega > \Pi^2$. Thus, $\sqrt{\Pi^2 - 4\Omega} > |\Pi| = -\Pi$. In this case, $\Pi + \sqrt{\Pi^2 - 4\Omega} > 0$ and $\Pi - \sqrt{\Pi^2 - 4\Omega} < 0$. We then know that $\lambda_+ = \pm a$, where a is a positive real number; $\lambda_- = \pm di$, where d is a positive real number. So, the equilibrium point is an unstable point.

In Row 6, because $\Omega = 0$, we have

$$\lambda_{\pm}^2 = \frac{\Pi \pm |\Pi|}{2}.$$

Because $\Pi < 0$, $\lambda_+^2 = 0$ and $\lambda_-^2 = \Pi < 0$. Thus, $\lambda_+ = 0$ and λ_- is pure imaginary. So in this case, the equilibrium point is a neutrally stable point.

In Row 7, because $\Omega > 0$, we have $\Pi^2 - 4\Omega < \Pi^2$. Therefore, $\sqrt{\Pi^2 - 4\Omega} < |\Pi| = -\Pi$. In this case, $\Pi + \sqrt{\Pi^2 - 4\Omega} < 0$ and $\Pi - \sqrt{\Pi^2 - 4\Omega} < 0$. Both λ_+ and λ_- are pure imaginary. So, the equilibrium point is a neutrally stable point.

In Row 8, because $\Pi = 0$, we have

$$\lambda_+^2 = \frac{\sqrt{-4\Omega}}{2} \quad \text{and} \quad \lambda_-^2 = \frac{-\sqrt{-4\Omega}}{2}.$$

Since $\Omega < 0$, thus $\lambda_+^2 > 0$ and $\lambda_-^2 < 0$. We then have that $\lambda_+ = \pm a$, where a is a positive real number; $\lambda_- = \pm di$, where d is a positive real number. So, the equilibrium point is an unstable point.

In Row 9 and 10, Condition C contradicts with Condition A after we use Condition B: $\Pi = 0$. Thus, these two are impossible.

In Row 11, because $\Omega < 0$, we have $\Pi^2 - 4\Omega > \Pi^2$. Thus, $\sqrt{\Pi^2 - 4\Omega} > |\Pi| = \Pi$. In this case, $\Pi + \sqrt{\Pi^2 - 4\Omega} > 0$ and $\Pi - \sqrt{\Pi^2 - 4\Omega} < 0$. We then know that $\lambda_+ = \pm a$, where a is a positive real number; $\lambda_- = \pm di$, where d is a positive real number. So, the equilibrium point is an unstable point.

In Row 12, because $\Omega = 0$, we have

$$\lambda_{\pm}^2 = \frac{\Pi \pm |\Pi|}{2}.$$

Because $\Pi > 0$, $\lambda_+^2 = \Pi$ and $\lambda_-^2 = 0$. Thus, $\lambda_+ = \pm\sqrt{\Pi}$ and $\lambda_- = 0$. So in this case, the equilibrium point is unstable.

In Row 13, because $\Omega > 0$, we have $\Pi^2 - 4\Omega < \Pi^2$. Therefore, $\sqrt{\Pi^2 - 4\Omega} < |\Pi| = \Pi$. In this case, $\Pi + \sqrt{\Pi^2 - 4\Omega} > 0$ and $\Pi - \sqrt{\Pi^2 - 4\Omega} > 0$. Both λ_+ and λ_- are real and one of their roots is positive. So, the equilibrium point is unstable.

In general, from the above analysis, there are two categories: (i) when all the four eigenvalues' real parts are zero, the equilibrium point is neutrally stable, (ii) as long as one of the eigenvalues has a positive real part, the equilibrium point is unstable. For this system, it is impossible that all the four eigenvalues' real parts are negative. In Table 1, Row 2, 3, 6, 7 belong to the first category because their eigenvalues are either zero or pure imaginary. Row 1, 4, 5, 8, 11, 12, 13 belong to the second category because at least one of the eigenvalues is positive.

To make it convenient to use Table 1 in the future, the properties of λ_+^2 and λ_-^2 are indicated in the final two columns of the table. In that two columns, “c” means imaginary complex conjugate numbers, “+” means positive numbers, “-” means negative numbers, and “0” means zeroes.

As an example, when we set $M_b = T = 0.01$ and $\mu = 4/9$ in Model A, there are five equilibrium points on x -axis: $(-1.180392, 0)$, $(-0.060183, 0)$, $(-0.000137, 0)$, $(0.118920, 0)$, $(1.218591, 0)$. We find that only $(-0.000137, 0)$ belongs to the first category and is neutrally stable. All the others belong to the second category and is unstable.

5. Concluding Remarks

We have studied the existence of new equilibrium points for our system. In addition to the usual equilibrium points, we find that there are some new equilibrium points for particular parameter space. We provide two models in this paper. One is an analytic model from Miyamoto & Nagai (1975) (Model A) and another is a model of power-law density profile (Model B). Since there is no analytic formula for the power-law density profile, we have to study this model numerically. For Model A, we have some interesting analytic results and they are consistent with the numerical results. The new equilibrium points only exist on the x -axis for Model A. However, for Model B, we can have new equilibrium points both on the vertical line: $x = 1/2 - \mu$ and the x -axis.

Our study implies that the structure of constant potential contour might be more complicated due to the existence of new equilibrium points. The stability could be different according to the linear analysis in the previous section. Thus, the dynamics around a binary system might become very different when the influence of a belt is included.

Acknowledgment

We are grateful to the National Center for High-performance Computing for computer time and facilities. This work is supported in part by the National Science Council, Taiwan, under Li-Chin Yeh's Grants NSC 94-2115-M-134-002 and also Ing-Guey Jiang's Grants NSC 94-2112-M-008-010.

REFERENCES

Brent, R. P., 1973, Algorithms for Minimization without Derivatives, Englewood Cliffs, NJ: Prentice-Hall.

Chermnykh, S. V., 1987, Vest. Leningrad Univ. 2, 10.

Jiang, I.-G., Yeh, L.-C., 2003, Int. J. Bifurcation and Chaos, 13, 617.

Jiang, I.-G., Yeh, L.-C., 2004, Int. J. Bifurcation and Chaos, 14, 3153.

Jiang, I.-G., Yeh, L.-C., 2006, Astrophysics and Space Science, accepted.

Miyamoto, M., Nagai, R., 1975, Publ. Astron. Soc. Japan, 27, 533.

Lizano, S., Shu, F. H., 1989, ApJ, 342, 834.

Papadakis, K. E., 2004, A&A, 425, 1133.

Papadakis, K. E., 2005a, Astrophysics and Space Science, 299, 67.

Papadakis, K. E., 2005b, Astrophysics and Space Science, 299, 129.

Press, W. H. et al., 1992, Numerical recipes in Fortran, Cambridge University Press.

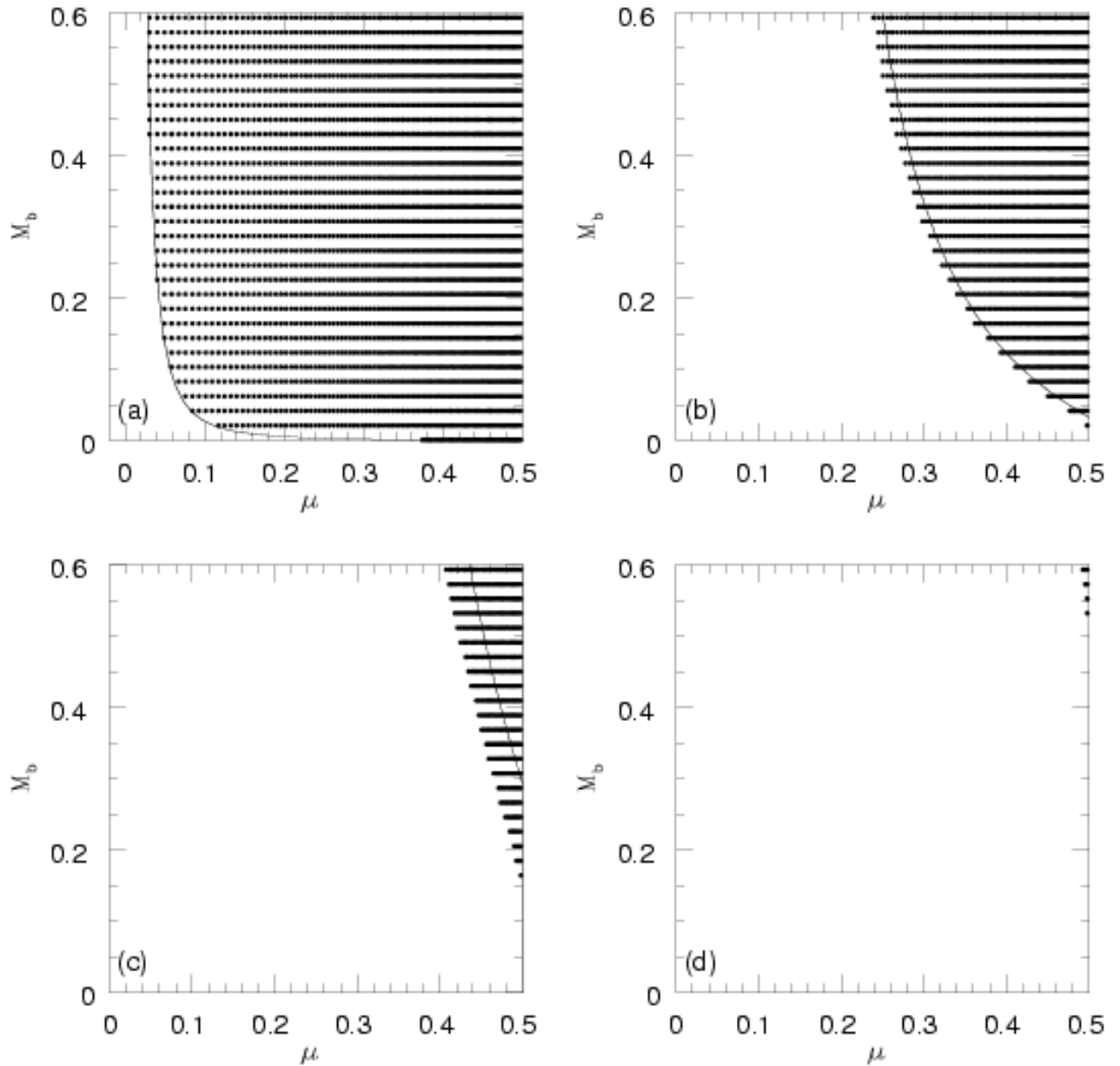


Fig. 1.— The existence area of new equilibrium points on the $\mu - M_b$ plane for Model A. In (a) $T = 0.01$; (b) $T = 0.1$; (c) $T = 0.2$ and (d) $T = 0.3$ (please see the main text for more details).

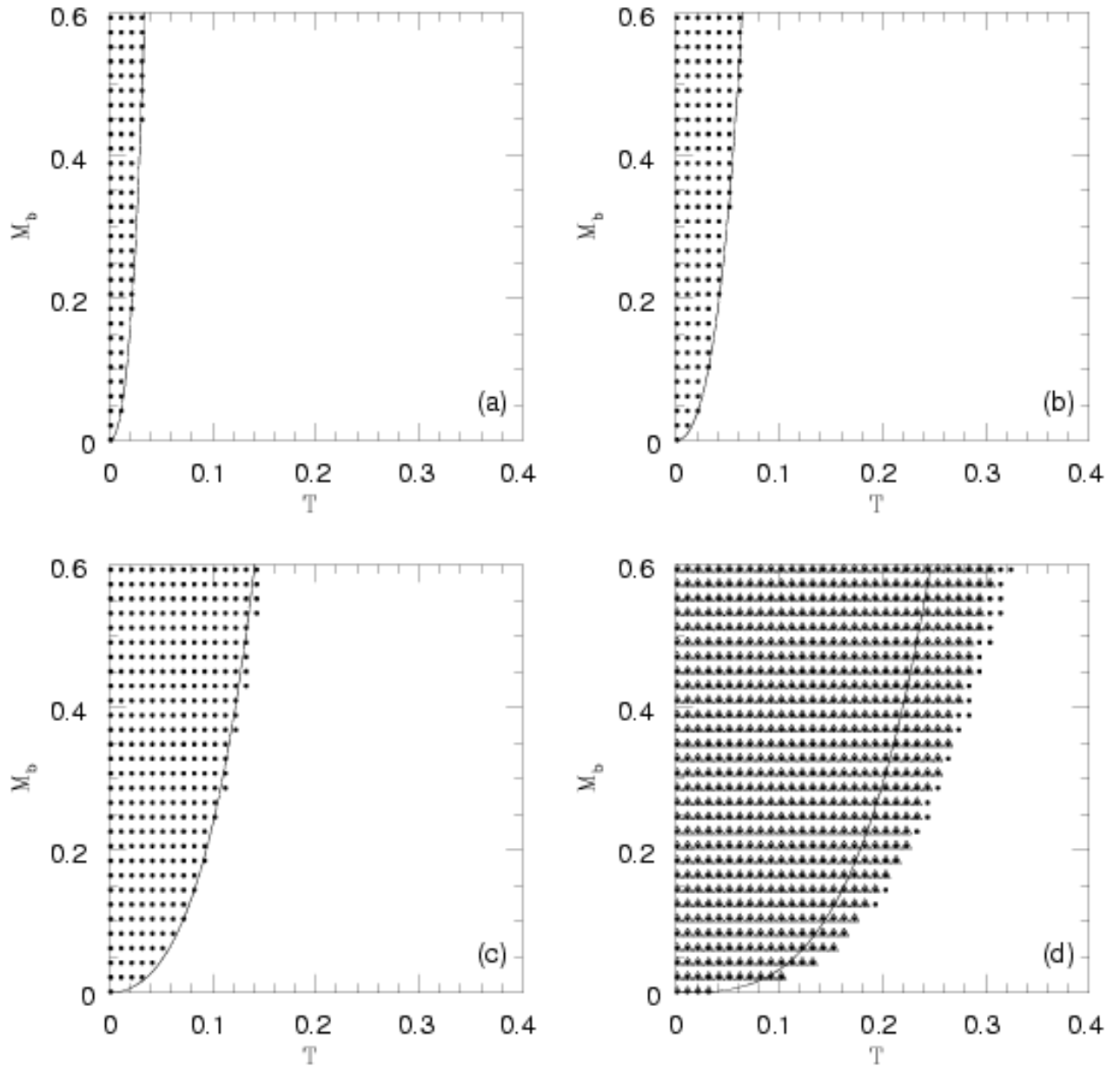


Fig. 2.— The existence area of new equilibrium points on the $T - M_b$ plane for Model A. In (a) $\mu = 1/11$; (b) $\mu = 1/6$; (c) $\mu = 1/3$ and (d) $\mu = 1/2$ (please see the main text for more details).

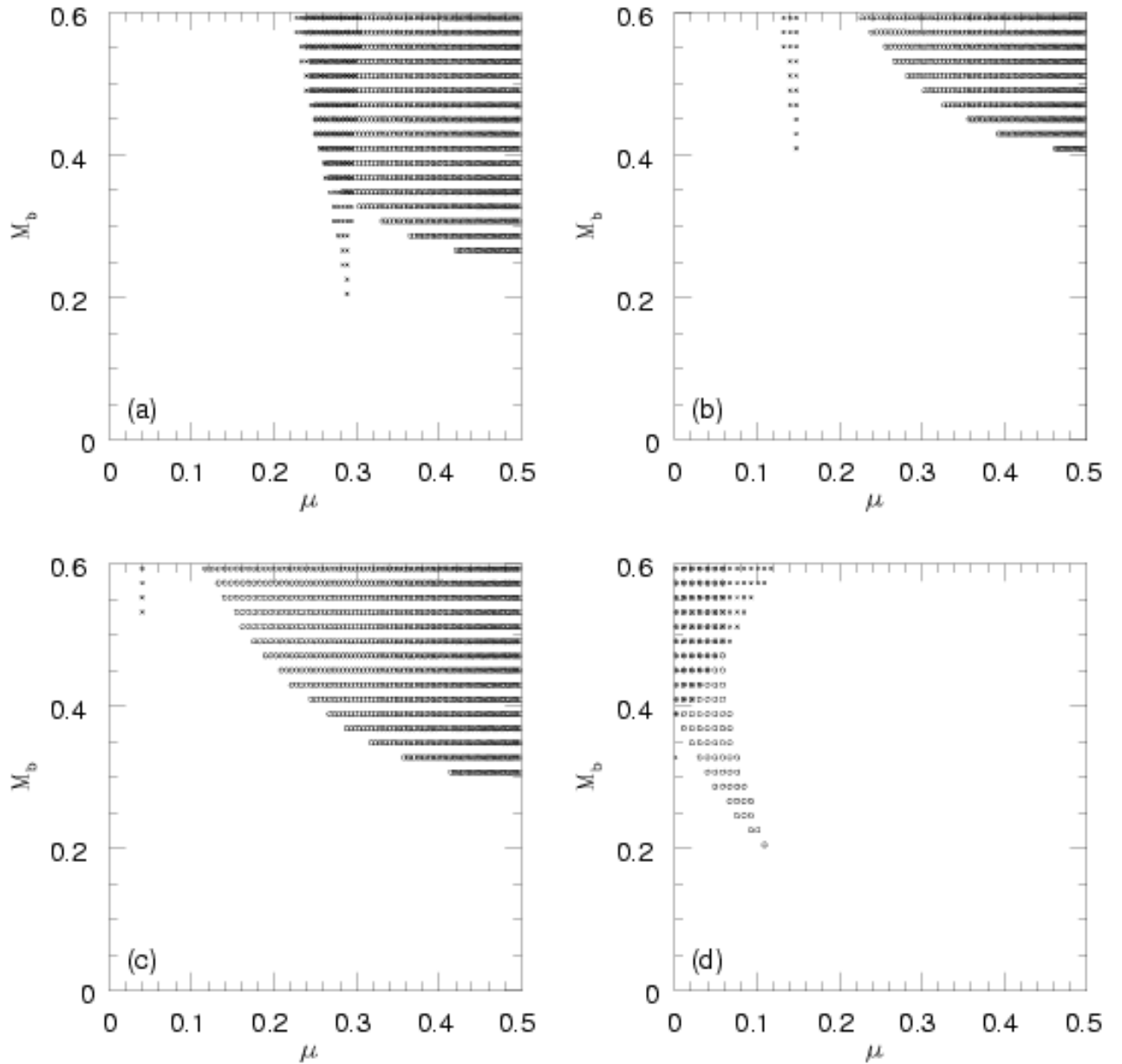


Fig. 3.— The existence area of new equilibrium points on the $\mu - M_b$ plane for Model B. In (a) $r_i = 0.2$; (b) $r_i = 0.4$; (c) $r_i = 0.6$ and (d) $r_i = 0.8$ (please see the main text for more details).

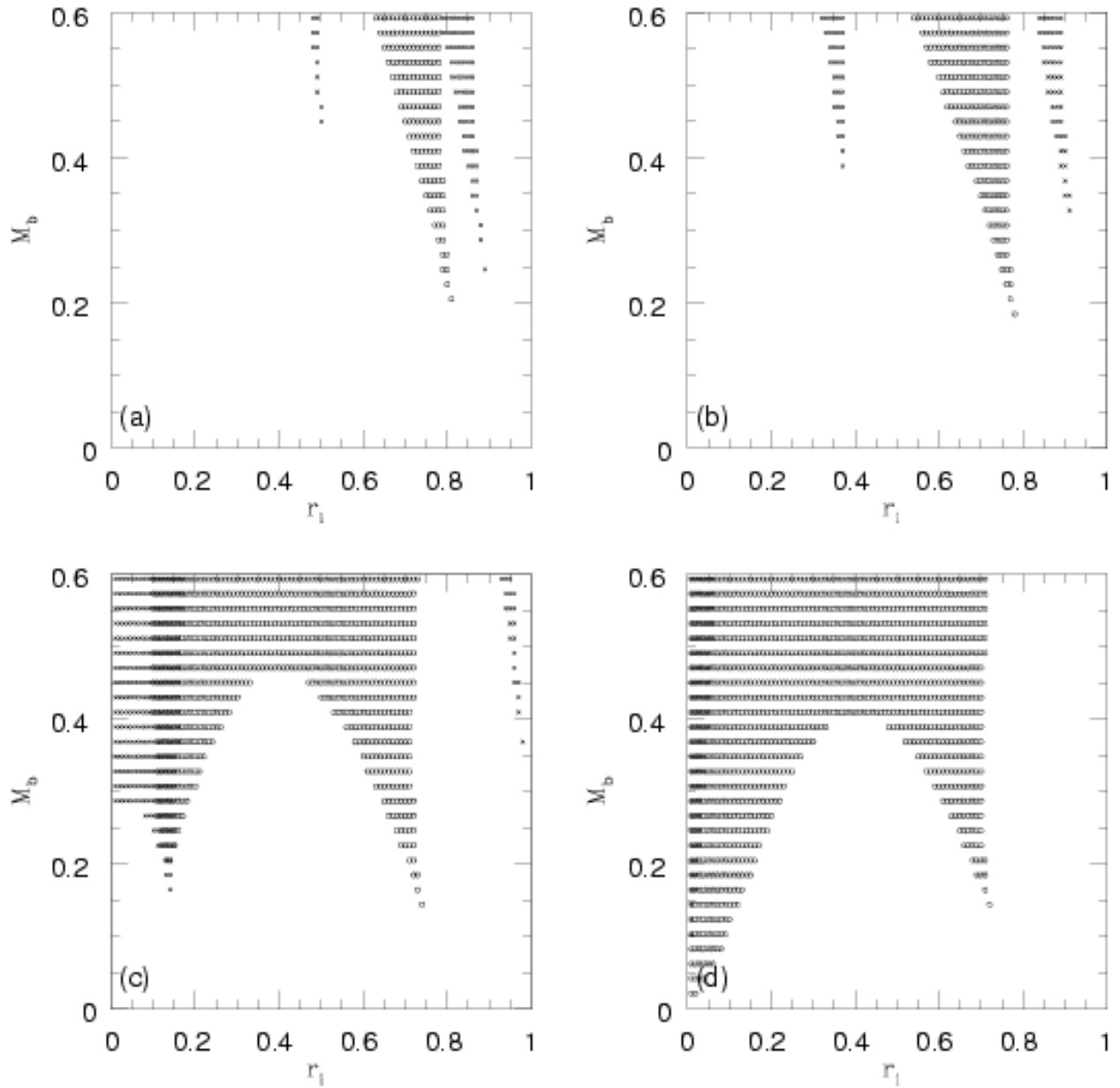


Fig. 4.— The existence area of new equilibrium points on the $r_i - M_b$ plane for Model B. In (a) $\mu = 1/11$; (b) $\mu = 1/6$; (c) $\mu = 1/3$ and (d) $\mu = 1/2$ (please see the main text for more details).